10068 *Inorg. Chem.* **2009**, *48*, 10068–10077
DOI: 10.1021/ic9009306

Inorganic Chemistry
Article

Organo-Ruthenium Supported Heteropolytungstates: Synthesis, Structure, Electrochemistry, and Oxidation Catalysis

Li-Hua Bi,[†,⊥] Ghada Al-Kadamany,[†] Elena V. Chubarova,[†,¶] Michael H. Dickman,[†] Lifang Chen,[†,⊗] Divakara S. Gopala,[†,⊗] Ryan M. Richards,[*,†,⊗] Bineta Keita,[‡] Louis Nadjo,[‡] Helge Jaensch,[§] Georges Mathys,[∥] and Ulrich Kortz[*,†]

[†] *Jacobs University, School of Engineering and Science, P.O. Box 750 561, 28725 Bremen, Germany,* [‡] *Laboratoire de Chimie Physique, UMR 8000, CNRS, Equipe d'Electrochimie et Photoélectrochimie, Université Paris-Sud, Bâtiment 350, 91405 Orsay Cedex, France,* [§] *ExxonMobil Catalyst Technologies LLC, 4500 Bayway Drive, Baytown, Texas 77522, and* [∥] *ExxonMobil Chemical Europe Inc., Hermeslaan 2, B-1831 Machelen, Belgium and Department of Chemistry and Geochemistry, Colorado School of Mines, 1500 Illinois, Golden, Colorado 80401.* [⊥] *Current address: College of Chemistry, Jilin University, Changchun, 130012, P.R. China.* [¶] *Current address: Biomedical and X-ray Physics, Department of Applied Physics, Royal Institute of Technology, S-10691 Stockholm, Sweden.* [⊗] *Current address: Colorado School of Mines, Department of Chemistry and Geochemistry, 304 Coolbaugh Hall, 1500 Illinois St, Golden, CO 80401, U.S.A.*

Received May 12, 2009

The reaction of $[Ru(arene)Cl_2]_2$ (arene = benzene, *p*-cymene) with $[X_2W_{22}O_{74}(OH)_2]^{12-}$ ($X = Sb^{III}$, Bi^{III}) in buffer medium resulted in four organo-ruthenium supported heteropolytungstates, $[Sb_2W_{20}O_{70}(RuC_6H_6)_2]^{10-}$ (**1**), $[Bi_2W_{20}O_{70}(RuC_6H_6)_2]^{10-}$ (**2**), $[Sb_2W_{20}O_{70}(RuC_{10}H_{14})_2]^{10-}$ (**3**), and $[Bi_2W_{20}O_{70}(RuC_{10}H_{14})_2]^{10-}$ (**4**), which have been characterized in solution by multinuclear (^{183}W, ^{13}C, ^{1}H) NMR, UV−vis spectroscopy, electrochemistry, and in the solid state by single-crystal X-ray diffraction, IR spectroscopy, thermogravimetric analysis, and elemental analysis. Polyanions **1**, **2**, and **4** crystallize in the triclinic system, space group $P\bar{1}$ with the following unit cell parameters: $K_5Na_5[Sb_2W_{20}O_{70}(RuC_6H_6)_2]\cdot 22H_2O$ (**KNa-1**), $a = 12.1625(2)$ Å, $b = 13.1677(2)$ Å, $c = 16.0141(3)$ Å, $\alpha = 78.9201(7)°$, $\beta = 74.4442(8)°$, $\gamma = 78.9019(8)°$, and $Z = 1$; $Cs_2Na_8[Bi_2W_{20}O_{70}(RuC_6H_6)_2]\cdot 30H_2O$ (**CsNa-2**), $a = 11.6353(7)$ Å, $b = 13.3638(7)$ Å, $c = 16.7067(8)$ Å, $\alpha = 79.568(2)°$, $\beta = 71.103(2)°$, $\gamma = 80.331(2)°$, and $Z = 1$; $Na_{10}[Bi_2W_{20}O_{70}(RuC_{10}H_{14})_2]\cdot 35H_2O$ (**Na-4**), $a = 15.7376(12)$ Å, $b = 15.9806(13)$ Å, $c = 24.2909(19)$ Å, $\alpha = 92.109(4)°$, $\beta = 101.354(4)°$, $\gamma = 97.365(3)°$, and $Z = 2$. Polyanions **1**−**4** consist of two $(L)Ru^{2+}$ (L = benzene or *p*-cymene) units linked to a $[X_2W_{20}O_{70}]^{14-}$ ($X = Sb^{III}$, Bi^{III}) fragment via Ru−O(W) bonds resulting in an assembly with idealized C_{2h} symmetry. Polyanions **1**−**4** are stable in solution as indicated by the expected ^{183}W, ^{13}C, and ^{1}H NMR spectra. The electrochemistry of **1**−**4** is described by considering the reduction and the oxidation processes. The nature of the arene in Ru(arene) has practically no influence on the formal potentials of the W-centers, which are more sensitive to the Sb or Bi hetero atoms. The results suggest that the respective Sb- and Bi derivatives have very different pK_a values, with the reduced form of **1** being the most basic, thus permitting the observation of two well-developed voltammetric waves at pH 6. In contrast, the identity of the arene influences the oxidation processes, thus permitting to distinguish them. A strong electrocatalytic water oxidation peak is observed that is more positive than the one corresponding to the Ru(arene) oxidation process. Also a stepwise oxidation of the Ru(benzene) group could be observed at pH 3. The catalytic efficiency, on the other hand, of **1**−**4** toward the oxidation of *n*-hexadecane and *p*-xylene illustrated the effect of ruthenium substitution on the polyanion catalytic performance.

Introduction

Polyoxometalates (POMs) constitute a large and distinct class of molecular metal−oxygen clusters with a fascinating structural variety combined with remarkable chemical properties.[1] The existence of POMs has been known for almost 200 years, and new anions with different size, composition, and structure are still being discovered.[2−6] The significant contemporary interest in POM chemistry is driven by perceived and realized applications in many areas such as analytical sciences, materials science, catalysis, medicine, and in the emerging areas of bio- as well as nanotechnology.[7]

*To whom correspondence should be addressed. E-mail: u.kortz@jacobs-university.de (U.K.), rrichard@mines.edu (R.M.R.). Fax: +49-421-200 3229 (U.K.), +1 303 273 3629 (R.M.R.).

 Published on Web 09/25/2009

To date more than 70 different elements have been discovered as constituents of heteropolyanions. Most POMs are composed of early transition metal MO_6 ($M = W^{6+}$, Mo^{6+}, etc.) octahedra and main group XO_4 ($X = P^V$, Si^{IV}, etc.) tetrahedra. The most famous POMs are probably the Keggin (e.g., $[PW_{12}O_{40}]^{3-}$) and the Wells−Dawson (e.g., $[P_2W_{18}O_{62}]^{6-}$) ions. However, POMs containing a hetero group with a lone pair of electrons (e.g., Sb^{III}, Bi^{III}) have also been known for a long time. The fact that the lone pair of electrons on the heteroatom does not allow the closed Keggin unit to form has resulted in some unexpected structures, e.g. $[NaSb_9W_{21}O_{86}]^{18-}$ and $[Na_2Sb_8W_{36}O_{132}(H_2O)_4]^{22-}$.[8] A class of sandwich-type POMs based on two lone-pair containing, β-Keggin fragments, e.g. $[\beta\text{-}Sb^{III}W_9O_{33}]^{9-}$ and $[\beta\text{-}Bi^{III}W_9O_{33}]^{9-}$ has emerged. The first members of this class, $([M_2(H_2O)_6(WO_2)_2(\beta\text{-}SbW_9O_{33})_2]^{(14-2n)-}$ ($M^{n+} = Mn^{2+}$, Fe^{3+}, Co^{2+}, Ni^{2+}), were reported by Krebs et al. in 1997.[8b] Since then some more isostructural derivatives have been characterized, such as $[M_2(H_2O)_6(WO_2)_2(\beta\text{-}XW_9O_{33})_2]^{(14-2n)-}$ ($X = Bi^{III}$, Sb^{III}; $M^{n+} = Fe^{3+}, Co^{2+}, Zn^{2+}$), $[M_3(H_2O)_8(WO_2)(\beta\text{-}TeW_9O_{33})_2]^{8-}$ ($M = Zn^{2+}$, Co^{2+}, Ni^{2+}), $[Cu_3(H_2O)_3(BiW_9O_{33})_2]^{12-}$ and $[M_4(H_2O)_{10}(\beta\text{-}XW_9O_{33})_2]^{n-}$ ($n = 6$, $X = As^{III}$ and Sb^{III}, $M = Fe^{3+}$ and Cr^{3+}; $n = 4$, $X = Se^{IV}$, Te^{IV}, $M = Fe^{3+}$ and Cr^{3+}; $n = 8$, $X = Se^{IV}$, Te^{IV}, $M = Mn^{2+}$, Co^{2+}, Ni^{2+}, Zn^{2+}, Cd^{2+}, Hg^{2+} and $n = 10$, $X = Bi^{III}$, $M = Cu^{2+}$).[9]

The catalytic efficiency of ruthenium complexes for various organic transformations[10] has triggered attempts to synthesize ruthenium-containing POMs. Their high reactivity and selectivity toward the catalytic oxidation of a variety of organic substrates by O_2 and H_2O_2 were confirmed in the past few years.[11] The most common ruthenium sources for Ru-POM synthesis have been $RuCl_3 \cdot nH_2O$, $[Ru(H_2O)_6][C_7H_7SO_3]_2$, $Ru(acac)_3$ and *cis*-$Ru(dmso)_4Cl_2$.[12] For example, $[O\{Ru^{IV}Cl(\alpha_2\text{-}P_2W_{17}O_{61})\}_2]^{16-}$, $[WZnRu^{III}_2(OH)(H_2O)(ZnW_9O_{34})_2]^{11-}$, $[SiW_{11}Ru^{III}O_{39}(H_2O)]^{5-}$ and $[\{Ru_4O_4(OH)_4(H_2O)_4\}(\gamma\text{-}SiW_{10}O_{36})_2]^{10-}$ have been reported.[13] In 2004, our group published the structures of several $Ru^{II}(dmso)_3$-supported heteropolytungstates.[14] We also discovered that dmso inhibits the desired redox liability of the ruthenium centers. Thus we moved to organo-ruthenium precursors (e.g., $[(benzene)RuCl_2]_2$, $[(p\text{-cymene})RuCl_2]_2$) and reacted those

(1) (a) Pope, M. T. *Heteropoly and Isopoly Oxometalates*; Springer-Verlag: Berlin, 1983. (b) Pope, M. T.; Müller, A. *Angew. Chem., Int. Ed. Engl.* **1991**, *30*, 34. (c) *Polyoxometalates: From Platonic Solids to Anti-Retrociral Activity*; Pope, M. T., Müller, A., Eds.; Kluwer: Dordrecht, The Netherlands, 1994. (d) Müller, A.; Reuter, H.; Dillinger, S. *Angew. Chem., Int. Ed. Engl.* **1995**, *34*, 2328. (e) Hill, C. Polyoxometalates; *Chem. Rev.* **1998** (special thematic issue on polyoxometalates).

(2) (a) Müller, A.; Zhou, Y. -S.; Zhang, L. -J.; Bogge, H; Schmidtmann, M.; Dressel, M.; van Slageren, J. *Chem. Commun.* **2004**, 2038. (b) Müller, A.; Roy, S. *Coord. Chem. Rev.* **2003**, *245*, 153. (c) Müller, A.; Das, S. K.; Talismanov, S.; Roy, S.; Beckmann, E.; Bögge, H.; Schmidtmann, M.; Merca, A.; Berkle, A.; Allouche, L.; Zhou, Y. -S.; Zhang, L. -J. *Angew. Chem., Int. Ed.* **2003**, *42*, 5039. (d) Nyman, M.; Bonhomme, F.; Alam, T. M.; Parise, J. B.; Vaughan, G. M. B. *Angew. Chem., Int. Ed.* **2004**, *43*, 2787. (e) Wassermann, K.; Dickman, M. H.; Pope, M. T. *Angew. Chem., Int. Ed. Engl.* **1997**, *36*, 1445.

(3) (a) Cao, R.; Ma, H. Y.; Geletii, Y. V.; Hardcastle, K. I.; Hill, C. L. *Inorg. Chem.* **2009**, *48*, 5596. (b) Geletii, Y. V.; Huang, Z. Q.; Hou, Y.; Musaev, D. G.; Lian, T. Q.; Hill, C. L. *J. Am. Chem. Soc.* **2009**, *131*, 7522. (c) Kuznetsov, A. E.; Geletii, Y. V.; Hill, C. L.; Morokuma, K.; Musaev, D. G. *J. Am. Chem. Soc.* **2009**, *131*, 6844. (d) Cao, R.; Anderson, T. M.; Hillesheim, D. A.; Kögerler, P.; Hardcastle, K. I.; Hill, C. L. *Angew. Chem., Int. Ed.* **2008**, *47*, 9380. (e) Luo, Z.; Kögerler, P.; Cao, R.; Hakim, I.; Hill, C. L. *Dalton Trans.* **2008**, 54. (f) Hou, Y.; Fang, X. K.; Hill, C. L. *Chem.—Eur. J.* **2007**, *13*, 9442. (g) Cao, R.; Anderson, T. M.; Piccoli, P. M. B.; Schultz, A. J.; Koetzle, T. F.; Geletii, Y. V.; Slonkina, E.; Hedman, B.; Hodgson, K. O.; Hardcastle, K. I.; Fang, X. K.; Kirk, M. L.; Knottenbelt, S.; Kögerler, P.; Musaev, D. G.; Morokuma, K.; Takahashi, M.; Hill, C. L. *J. Am. Chem. Soc.* **2007**, *129*, 11118. (h) Luo, Z.; Kögerler, P.; Cao, R.; Hill, C. L. *Inorg. Chem.* **2009**, *48*, 7812.

(4) (a) Compain, J. D.; Mialane, P.; Dolbecq, A.; Marrot, J.; Proust, A.; Nakatani, K.; Yu, P.; Sécheresse, F. *Inorg. Chem.* **2009**, *48*, 6222. (b) Compain, J. D.; Mialane, P.; Dolbecq, A.; Mbomekallé, I. M.; Marrot, J.; Sécheresse, F.; Rivière, E.; Rogez, G.; Wernsdorfer, W. *Angew. Chem., Int. Ed.* **2009**, *48*, 3077. (c) Peng, Z. -H. *Angew. Chem., Int. Ed.* **2004**, *43*, 930. (d) Zhu, Y.; Wang, L. S.; Hao, J.; Xiao, Z. C.; Wei, Y. G.; Wang, Y. *Cryst. Growth Des.* **2009**, *9*, 3509. (e) Dong, L. J.; Huang, R. D.; Wei, Y. G.; Chu, W. *Inorg. Chem.* **2009**, *48*, 7528. (f) Zhu, Y. L.; Wang, L. S.; Hao, J. A.; Yin, P. C.; Zhang, J.; Li, Q.; Zhu, L.; Wei, Y. G. *Chem.—Eur. J.* **2009**, *15*, 3076.

(5) (a) Zhao, J. W.; Zheng, S. T.; Lib, Z. H.; Yang, G. Y. *Dalton Trans.* **2009**, 1300. (b) Zhao, J. W.; Wang, C. M.; Zhang, J.; Zheng, S. T.; Yang, G. Y. *Chem.—Eur. J.* **2008**, *14*, 9223. (c) Wang, J. P.; Zhao, J. W.; Ma, P. T.; Ma, J. C.; Yang, L. P.; Bai, Y.; Li, M. X.; Niu, J. Y. *Chem. Commun.* **2009**, 2362. (d) Ritchie, C.; Li, F. Y.; Pradeep, C. P.; Long, D. L.; Xu, L.; Cronin, L. *Dalton Trans.* **2009**, 6483. (e) Gao, G. G.; Li, F. Y.; Xu, L.; Liu, X. Z.; Yang, Y. Y. *J. Am. Chem. Soc.* **2008**, *130*, 10838. (f) Zhao, X. Y.; Liang, D. D.; Liu, S. X.; Sun, C. Y.; Cao, R. G.; Gao, C. Y.; Ren, Y. H.; Su, Z. M. *Inorg. Chem.* **2008**, *47*, 7133. (g) Lan, Y. Q.; Li, S. L.; Wang, X. L.; Shao, K. Z.; Du, D. Y.; Zang, H. Y.; Su, Z. M. *Inorg. Chem.* **2008**, *47*, 8179. (h) Tian, A. X.; Ying, J.; Peng, J.; Sha, J. Q.; Pang, H. J.; Zhang, P. P.; Chen, Y.; Zhu, M.; Su, Z. M. *Inorg. Chem.* **2009**, *48*, 100. (i) Zhang, C.; Howell, R. C.; Scotland, K. B.; Perez, F. G.; Todaro, L.; Francesconi, L. C. *Inorg. Chem.* **2004**, *43*, 7691. (j) San Felices, L.; Vitoria, P.; Gutiérrez-Zorrilla, J. M.; Reinoso, S.; Etxebarria, J.; Lezama, L. *Chem.—Eur. J.* **2004**, *10*, 5138.

(6) (a) Kortz, U.; Savelieff, M. G.; Bassil, B. S.; Dickman, M. H. *Angew. Chem., Int. Ed.* **2001**, *40*, 3384. (b) Kortz, U.; Hamzeh, S. S.; Nasser, N. A. *Chem.—Eur. J.* **2003**, *9*, 2945. (c) Hussain, F.; Bassil, B. S.; Bi, L.-H; Reicke, M.; Kortz, U. *Angew. Chem., Int. Ed.* **2004**, *43*, 3485. (d) Bi, L.-H.; Reicke, M.; Kortz, U.; Keita, B.; Nadjo, L.; Clark, R. J. *Inorg. Chem.* **2004**, *43*, 3915. (e) Bi, L.-H.; Kortz, U.; Keita, B.; Nadjo, L.; Borrmann, H. *Inorg. Chem.* **2004**, *43*, 8367. (f) Kortz, U.; Hussain, F.; Reicke, M. *Angew. Chem., Int. Ed.* **2005**, *44*, 3773. (g) Bassil, B. S.; Nellutla, S.; Kortz, U.; Stowe, A. C.; van Tol, J.; Dalal, N. S.; Keita, B.; Nadjo, L. *Inorg. Chem.* **2005**, *44*, 2659. (h) Bi, L.-H.; Kortz, U.; Nellutla, S.; Stowe, A. C.; Dalal, N. S.; Keita, B.; Nadjo, L. *Inorg. Chem.* **2005**, *44*, 896. (i) Mal, S. S.; Kortz, U. *Angew. Chem., Int. Ed.* **2005**, *44*, 3777. (j) Bi, L.-H.; Kortz, U.; Keita, B.; Nadjo, L.; Daniels, L. *Eur. J. Inorg. Chem.* **2005**, 3034. (k) Izarova, N. V.; Dickman, M. H.; Biboum, R. N.; Keita, B.; Nadjo, L.; Ramachandran, V.; Dalal, N. S.; Kortz, U. *Inorg. Chem.* **2009**, *48*, 7504. (l) Nsouli, N. H.; Ismail, A. H.; Helgadottir, I. S.; Dickman, M. H.; Clemente-Juan, J. M.; Kortz, U. *Inorg. Chem.* **2009**, *48*, 5884. (m) Bi, L. H.; Dickman, M. H.; Kortz, U. *CrystEngComm.* **2009**, *11*, 965.

(7) (a) *Polyoxometalate Chemistry: From Topology via Self-Assembly to Applications*; Pope, M. T., Müller, A., Eds.; Kluwer: Dordrecht, The Netherlands, 2001. (b) *Polyoxometalate Chemistry for Nano-Composite Design*; Yamase, T.; Pope, M. T., Eds.; Kluwer: Dordrecht, The Netherlands, 2002. (c) Pope, M. T. *Comp. Coord. Chem. II* **2003**, *4*, 635. (d) Hill, C. L. *Comp. Coord. Chem. II* **2003**, *4*, 679. (e) *Polyoxometalate Molecular Science*; Borrás-Almenar, J. J., Coronado, E., Müller, A., Pope, M. T., Eds.; Kluwer: Dordrecht, The Netherlands, 2004. (f) Casan-Pastor, N.; Gomez-Romero, P. *Front. Biosci.* **2004**, *9*, 1759. (g) Yin, C. X.; Finke, R. G. *J. Am. Chem. Soc.* **2005**, *127*, 9003. (h) Chen, L. F.; Hu, J. C.; Mal, S. S.; Kortz, U.; Jaensch, H.; Mathys, G.; Richards, R. M. *Chem.—Eur. J.* **2009**, *15*, 7490.

(8) (a) Fisher, J.; Ricard, L.; Weiss, R. *J. Am. Chem. Soc.* **1976**, *98*, 3050. (b) Bösing, M.; Loose, I.; Pohlmann, H.; Krebs, B. *Chem.—Eur. J.* **1997**, *3*, 1232.

(9) (a) Loose, I.; Droste, E.; Bösing, M.; Pohlmann, H.; Dickman, M. H.; Roşu, C.; Pope, M. T.; Krebs, B. *Inorg. Chem.* **1999**, *38*, 2688. (b) Rusu, D.; Roşu, C.; Crăciun, C.; David, L.; Rusu, M.; Marcu, G. *J. Mol. Struct.* **2001**, *563−564*, 427. (c) Kortz, U.; Savelieff, M. G.; Bassil, B. S.; Keita, B.; Nadjo, L. *Inorg. Chem.* **2002**, *41*, 783. (d) Limanski, E. M.; Drewes, D.; Droste, E.; Bohner, R.; Krebs, B. *J. Mol. Struct.* **2003**, *656*, 17.

(10) Naota, T.; Takaya, H.; Murahashi, S. I. *Chem. Rev.* **1998**, *98*, 2599.

(11) (a) Neumann, R.; Khenkin, A. M.; Dahan, M. *Angew. Chem., Int. Ed. Engl.* **1995**, *34*, 1587. (b) Neumann, R.; Dahan, M. *Nature* **1997**, *388*, 353. (c) Neumann, R.; Dahan, M. *J. Am. Chem. Soc.* **1998**, *120*, 11969. (d) Bonchio, M.; Scorrano, G.; Toniolo, P.; Proust, A.; Artero, V.; Conte, V. *Adv. Synth. Catal.* **2002**, *344*, 841. (e) Yamaguchi, K.; Mizuno, N. *New J. Chem.* **2002**, *26*, 972. (f) Adam, W.; Alsters, P. L.; Neumann, R.; Saha-Möller, C. R.; Seebach, D.; Beck, A. K.; Zhang, R. J. *Org. Chem.* **2003**, *68*, 8222. (g) Yin, C. X.; Finke, R. G. *Inorg. Chem.* **2005**, *44*, 4175.

(12) (a) Rong, C. Y.; Pope, M. T. *J. Am. Chem. Soc.* **1992**, *114*, 2932. (b) Higashijima, M. *Chem. Lett.* **1999**, 1093. (c) Alessandro, B.; Bonchio, M.; Sartorel, A; Scorrano, G. *Eur. J. Inorg. Chem.* **2000**, 17. (d) Nomiya, K.; Torii, H.; Nomura, K.; Sato, Y. *J. Chem. Soc., Dalton Trans.* **2001**, 1506. (e) Sadakane, M.; Higashijima, M. *Dalton Trans.* **2003**, 659. (f) Khenkin, A. M.; Shimon, L. J. W.; Neumann, R. *Inorg. Chem.* **2003**, *42*, 3331. (g) Bi, L. H.; Hussain, F.; Kortz, U.; Sadakane, M.; Dickman, M. H. *Chem. Commun.* **2004**, 1420.

with a large variety of lacunary polytungstates. We successfully synthesized organo-Ru(II)-supported lacunary tungstosilicates and -germanates, $[(RuC_6H_6)_2XW_9O_{34}]^{6-}$ (X = Si, Ge) and $[\{Ru(C_6H_6)(H_2O)\}\{Ru(C_6H_6)\}(\gamma\text{-}XW_{10}O_{36})]^{4-}$ (X = Si, Ge), lacunary tungstoarsenate and tungstophosphate $[(RuC_6H_6)XW_9O_{34}]^{7-}$ (X = P, As), zinc-substituted tungstoarsenate, and a derivative of the cyclic $[H_7P_8W_{48}O_{184}]^{33-}$ anion, $[\{K(H_2O)\}_3\{Ru(p\text{-cymene})(H_2O)\}_4P_8W_{49}O_{186}(H_2O)_2]^{27-}$.[15] Before us some other groups reported on organometallic-ruthenium POMs structures, most of them being characterized by elemental analysis, IR, and multinuclear NMR.[16] In 2003, Proust and co-workers published the structure of the first carbene derivative of a Ru-containing heteropolytungstate, $[(PW_9O_{34})_2(cis\text{-}WO_2)(cis\text{-}RuL^{Me}{}_2)]^{13-}$ (L^{Me} = 1,3-dimethylimidazolidine-2-ylidene).[17] In 2005, the same group reported on the Keggin-based (arene)Ru^{2+} derivatives $[PW_{11}O_{39}\{Ru(arene)(H_2O)\}]^{5-}$ and $[\{PW_{11}O_{39}\{Ru(arene)\}\}_2\{WO_2\}]^{8-}$ (arene = benzene, toluene, *p*-cymene, hexamethylbenzene),[18] and also the first Ru-derivative with the Krebs-type structure, $[Sb_2W_{20}O_{70}\{Ru(p\text{-cymene})\}_2]^{10-}$.[19] In 2006, Sakai et al. reported on the Wells−Dawson derivatives $[\{(benzene)Ru(H_2O)(\alpha_2\text{-}P_2W_{17}O_{61})\}^{8-}$ and $[\{(p\text{-cymene})Ru(H_2O)\}(\alpha_2\text{-}P_2W_{17}O_{61})]^{8-}$,[20] and they also showed that these species can act as homogeneous catalyst precursors for the selective oxidations of a wide variety of alcohols with 1 atm molecular oxygen in water−alcohol biphasic media without any additives.[21]

Herein we present the synthesis, structure, electrochemistry and catalytic properties of four (arene)Ru^{2+} derivatives of the Krebs type $[X_2W_{22}O_{74}(OH)_2]^{12-}$ (X = Sb^{III}, Bi^{III}) structure.

Experimental Section

Synthesis. The polyanion precursors $Na_{12}[Sb_2W_{22}O_{74}(OH)_2]\cdot 41H_2O$ and $Na_{12}[Bi_2W_{22}O_{74}(OH)_2]\cdot 44H_2O$ were synthesized according to published procedures, and purity was confirmed by infrared spectroscopy.[8b,9a] All other reagents were used as purchased without further purification.

$K_5Na_5[Sb_2W_{20}O_{70}(RuC_6H_6)_2]\cdot 22H_2O$ (KNa-1). $[(C_6H_6)RuCl_2]_2$ (0.04 g; 0.08 mmol) and $Na_{12}[Sb_2W_{22}O_{74}(OH)_2]$ (0.5 g; 0.08 mmol) were dissolved with stirring and heating to 50 °C for 30 min in 20 mL of 0.5 M sodium acetate buffer (pH 6.0). The solution was cooled and then filtered. Then 0.5 mL of 1.0 M KCl solution was added to the filtrate which was left for slow evaporation. A dark red-brown crystalline product was collected by filtration (yield 0.22 g, 47%).

IR of **KNa-1**: 480 (w), 560 (sh), 601 (m), 768 (s), 841 (m), 882 (sh), 931 (s), 1436 (w), 1618 (m), 1638 (m) cm^{-1}.

Anal. Calcd (Found) for **KNa-1**: K 3.2 (2.6), Na 1.9 (1.9), W 60.2 (59.5), Ru 3.3 (2.9), Sb 4.0 (4.2), C 2.4 (2.4), H 0.9 (1.0).

NMR of **KNa-1** in D_2O at 293 K: ^1H: δ 6.1 ppm; ^{13}C: δ 80.8 ppm; ^{138}W: −58.4, −103.1, −115.8, −125.4, −157.3, and −334.1 ppm.

UV−vis (H_2O) [λ_{max} (ε)]: 436 (3.3×10^3 L·mol^{-1}·cm^{-1}), 359 (5.9×10^3 L·mol^{-1}·cm^{-1}), 280 nm (4.1×10^4 L·mol^{-1}·cm^{-1}).

$Cs_2Na_8[Bi_2W_{20}O_{70}(RuC_6H_6)_2]\cdot 30H_2O$ (CsNa-2). $[(C_6H_6)RuCl_2]_2$ (0.04 g; 0.08 mmol) and $Na_{12}[Bi_2W_{22}O_{74}(OH)_2]$ (0.5 g; 0.08 mmol) were dissolved with stirring and heating to 50 °C for 30 min in 20 mL of 0.5 M sodium acetate buffer (pH 6.0). The solution was cooled and then filtered. Then 0.5 mL of 1.0 M CsCl solution was added to the filtrate which was left for slow evaporation. A dark red crystalline product was collected by filtration (yield 0.23 g, 47%).

IR of **CsNa-2**: 459 (w), 518 (sh), 609 (sh), 647 (m), 745 (s), 800 (vs), 843 (sh), 943 (s), 1430 (w), 1630 (m) cm^{-1}.

Anal. Calcd (Found) for **CsNa-2**: Na 2.8 (2.8), W 56.0 (54.8), Ru 3.1 (2.8), Bi 6.4 (6.0), C 2.2 (2.6), H 1.1 (1.3).

NMR of **CsNa-2** in D_2O at 293 K: ^1H: δ 6.1 ppm; ^{13}C: δ 81.0 ppm; ^{138}W: −31.1, −88.8, −111.8, −125.1, −154.7, and −336.1 ppm.

UV−vis (H_2O) [λ_{max} (ε)]: 433 (3.0×10^3 L·mol^{-1}·cm^{-1}), 355 (5.3×10^3 L·mol^{-1}·cm^{-1}), 272 nm (3.6×10^4 L·mol^{-1}·cm^{-1}).

$Cs_3Na_7[Sb_2W_{20}O_{70}(RuC_{10}H_{14})_2]\cdot 27H_2O$ (CsNa-3). A 0.05 g (0.08 mmol) sample of $[(C_{10}H_{14})RuCl_2]_2$ was dissolved with stirring in 20 mL of 0.5 M sodium acetate buffer (pH 6.0). Then 0.5 g (0.08 mmol) of $Na_{12}[Sb_2W_{22}O_{74}(OH)_2]$ was added. The solution was stirred at room temperature for 2 h and filtered. Then 0.5 mL of 1.0 M CsCl solution was added to the filtrate which was left for slow evaporation. An orange crystalline product was collected by filtration (yield 0.18 g, 39%).

IR of **CsNa-3**: 457 (w), 667 (w), 703 (w), 769 (s), 807 (s), 845 (sh), 948 (s), 1642 (m) cm^{-1}.

Anal. Calcd (Found) for **CsNa-3**: Cs 6.1 (5.4), Na 2.5 (2.3), W 56.1 (55.3), Ru 3.1 (2.9), Sb 3.7 (3.8), C 3.7 (3.6), H 1.3 (1.3).

NMR of **CsNa-3** in D_2O at 293 K: ^1H: δ 1.38, 1.40, 2.34, 3.07, 5.61, 5.63, 6.18, 6.20 ppm; ^{13}C: δ 16.98, 17.05, 22.15, 30.55, 31.06, 75.79, 76.36, 83.22, 96.47, 99.05 ppm; ^{138}W: −71.9, −103.1, −118.8, −165.7, and −327.6 ppm.

UV−vis (H_2O) [λ_{max} (ε)]: 444 (3.0×10^3 L·mol^{-1}·cm^{-1}), 361 (5.5×10^3 L·mol^{-1}·cm^{-1}), 278 nm (4.1×10^4 L·mol^{-1}·cm^{-1}).

$Na_{10}[Bi_2W_{20}O_{70}(RuC_{10}H_{14})_2]\cdot 35H_2O$ (Na-4). $[(C_{10}H_{14})RuCl_2]_2$ (0.05 g; 0.08 mmol) and $Na_{12}[Bi_2W_{22}O_{74}(OH)_2]$ (0.5 g; 0.08 mmol) were dissolved with stirring and heating to 50 °C for 30 min in 20 mL of 0.5 M sodium acetate buffer (pH 6.0). The solution was cooled and then filtered. Then 0.5 mL of 1.0 M KCl solution was added to the filtrate which was left for slow evaporation. An orange crystalline product was collected by filtration (yield 0.18 g, 39%).

IR of **Na-4**: 645 (vw), 735 (vw), 797 (w), 820 (sh), 947 (m), 1380 (vw), 1454 (w), 1625 (s) cm^{-1}.

Anal. Calcd (Found) for **Na-4**: Na 3.5 (3.1), W 56.2 (55.5), Ru 3.1 (2.7), Bi 6.4 (6.1), C 3.7 (4.0), H 1.5 (1.3).

NMR of **Na-4** in D_2O at 293 K: ^1H: δ 1.39, 1.41, 2.36, 3.07, 5.63, 5.64, 6.21, 6.22 ppm; ^{13}C: δ 16.86, 17.05, 22.52, 30.91, 31.06, 76.13, 76.36, 84.11, 96.26, 98.43 ppm; ^{138}W: −43.8, −88.9, −113.6, −117.8, −159.9, and −330.8 ppm.

(13) (a) Randall, W. J.; Weakley, T. J. R.; Finke, R. G. *Inorg. Chem.* **1993**, *32*, 1068. (b) Neumann, R.; Khenkin, A. M. *Inorg. Chem.* **1995**, *34*, 5753. (c) Sadakane, M.; Tsukuma, D.; Dickman, M. H.; Bassil, B. S.; Kortz, U.; Capron, M.; Ueda, W. *Dalton Trans.* **2007**, 2833. (d) Geletii, Y.; Botar, B.; Kögerler, P.; Hillesheim, D.; Musaev, D.; Hill, C. L. *Angew. Chem., Int. Ed.* **2008**, *47*, 3896. (e) Sartorel, A.; Carraro, M.; Scorrano, G.; De Zorzi, R.; Geremia, S.; McDaniel, N. D.; Bernhard, S.; Bonchio, M. *J. Am. Chem. Soc.* **2008**, *130*, 5006. (f) Yamaguchi, S.; Uehara, K.; Kamata, K.; Yamaguchi, K.; Mizuno, N. *Chem. Lett.* **2008**, *37*, 328. (g) Morris, A. M.; Anderson, O. P.; Finke, R. G. *Inorg. Chem.* **2009**, *48*, 4411.

(14) (a) Bi, L.-H.; Kortz, U.; Keita, B.; Nadjo, L. *Dalton Trans.* **2004**, 3184. (b) Bi, L.-H.; Dickman, M. H.; Kortz, U.; Dix, I. *Chem. Commun.* **2005**, 3962. (c) Sadakane, M.; Tsukuma, D.; Dickman, M. H.; Bassil, B. S.; Kortz, U.; Higashijima, M.; Ueda, W. *Dalton Trans.* **2006**, 4271.

(15) (a) Bi, L.-H.; Kortz, U.; Dickman, M. H.; Keita, B.; Nadjo, L. *Inorg. Chem.* **2005**, *44*, 7485. (b) Bi, L.-H.; Chubarova, E. V.; Nsouli, N. H.; Dickman, M. H.; Kortz, U.; Keita, B.; Nadjo, L. *Inorg. Chem.* **2006**, *45*, 8575. (c) Bi, L. H.; Hou, G. F.; Li, B.; Wu, L. X.; Kortz, U. *Dalton Trans.* **2009**, 6345. (d) Bi, L. H.; Hou, G. F.; Wu, L. X.; Kortz, U. *CrystEngComm* **2009**, *11*, 1532. (e) Mal, S. S.; Nsouli, N. H.; Dickman, M. H.; Kortz, U. *Dalton Trans.* **2007**, 2627.

(16) (a) Attanasio, D.; Bachechi, F.; Suber, L. *Dalton Trans.* **1993**, 2373. (b) Day, V. W.; Eberspacher, T. A.; Klemperer, W. G.; Planalp, R. P.; Schiller, P. W.; Yagasaki, A.; Zhong, B. *Inorg. Chem.* **1993**, *32*, 1629. (c) Klemperer, W. G.; Zhong, B.-X. *Inorg. Chem.* **1993**, *32*, 5821. (d) Pohl, M.; Lin, Y.; Weakley, T. J. R.; Nomiya, K.; Kaneko, M.; Weiner, H.; Finke, R. G. *Inorg. Chem.* **1995**, *34*, 767.

(17) Artero, V.; Proust, A.; Herson, P.; Villain, F.; Moulin, C. C. D.; Gouzerh, P. *J. Am. Chem. Soc.* **2003**, *125*, 11156.

(18) Artero, V.; Laurencin, D.; Villanneau, R.; Thouvenot, R.; Herson, P.; Gouzerh, P.; Proust, A. *Inorg. Chem.* **2005**, *44*, 2826.

(19) Laurencin, D.; Villanneau, R.; Herson, P.; Thouvenot, R.; Jeannin, Y.; Proust, A. *Chem. Commun.* **2005**, 5524.

(20) Sakai, Y.; Shinohara, A.; Hayashi, K.; Nomiya, K. *Eur. J. Inorg. Chem.* **2006**, 163.

(21) Kato, C. N.; Shinohara, A.; Moriya, N.; Nomiya, K. *Catal. Commun.* **2006**, *7*, 413.

Table 1. Crystallographic Data of **KNa-1**, **CsNa-2**, and **Na-4**

	KNa-1	**CsNa-2**	**Na-4**
empirical formula	$K_5Na_5Ru_2Sb_2W_{20}C_{12}H_{56}O_{92}$	$Cs_2Na_8Ru_2Bi_2W_{20}C_{12}H_{72}O_{100}$	$Na_{10}Ru_2Bi_2W_{20}C_{20}H_{98}O_{105}$
formula weight	6105.6	6563.5	6545.9
space group (nb)	$P\bar{1}$ (2)	$P\bar{1}$ (2)	$P\bar{1}$ (2)
a (Å)	12.1625(2)	11.6353(7)	15.7376(12)
b (Å)	13.1677(2)	13.3638(7)	15.9806(13)
c (Å)	16.0141(3)	16.7067(8)	24.2909(19)
α (deg)	78.9201(7)	79.568(2)	92.109(4)
β (deg)	74.4442(8)	71.103(2)	101.354(4)
γ (deg)	78.9019(8)	80.331(2)	97.365(3)
volume (Å^3)	2397.59(7)	2400.4(2)	5928.0(8)
Z	1	1	2
density(calc)(Mg/m^3)	4.229	4.329	3.547
temperature (K)	173(2)	173(2)	173(2)
wavelength (Å)	0.71073	0.71073	0.71073
abs coeff (mm^{-1})	25.088	28.778	22.651
$R\,[I > 2\sigma(I)]^a$	0.0438	0.0641	0.0779
R_w(all data)^b	0.1255	0.1634	0.2388

^{a} $R = \sum||F_o| - |F_c||/\sum|F_o|$. ^{b} $R_w = [\sum w(F_o^2 - F_c^2)^2/\sum w(F_o^2)^2]^{1/2}$.

UV−vis (H_2O) [λ_{max} (ε)]: 433 (3.6×10^3 L·mol^{-1}·cm^{-1}), 357 nm (6.6×10^3 L·mol^{-1}·cm^{-1}), 274 (4.8×10^4 L·mol^{-1}·cm^{-1}).

Infrared spectra were recorded on KBr pellets using a Nicolet Avatar spectrophotometer. All NMR spectra were recorded on a 400 MHz JEOL ECX instrument at room temperature using D_2O as solvent. Thermogravimetric analyses were carried out on a TA Instruments SDT Q600 thermobalance with a 100 mL/min flow of nitrogen, and the temperature was ramped from 20 to 700 °C at a rate of 10 °C/min. UV−vis spectra were recorded on a Cary 100 Bio UV−visible spectrophotometer on 3.5×10^{-4} M solutions of the relevant polyanions. Matched 1.000 cm optical path quartz cuvettes were used. Elemental analyses were performed by Analytische Laboratorien, Lindlar, Germany.

X-ray Crystallography. A single crystal of each of the compounds **KNa-1**, **CsNa-2**, and **Na-4**, was mounted on a glass fiber for indexing and intensity data collection at 100 K on a Bruker D8 SMART APEX CCD single-crystal diffractometer using Mo Kα radiation (λ = 0.71073 Å). Direct methods were used to solve the structures and to locate the heavy atoms (SHELXS97). Then the remaining atoms were found from successive difference maps (SHELXL97). Routine Lorentz and polarization corrections were applied and an absorption correction was performed using the SADABS program.[22] Crystallographic data are summarized in Table 1.

Electrochemistry

General Methods and Materials. Pure water was used throughout. It was obtained by passing through a RiOs 8 unit followed by a Millipore-Q Academic purification set. The compositions of the various media were as follows: for pH 3: 0.4 M CH_3COONa + $CH_2ClCOOH$; for pH 5 and pH 6: 0.4 M CH_3COONa + CH_3COOH.

Electrochemical Experiments. The polyanion concentration was 2×10^{-4} M, unless otherwise indicated. The solutions were deaerated thoroughly for at least 30 min with pure argon and kept under a positive pressure of this gas during the experiments. The source, mounting, and polishing of the glassy carbon (GC, Tokai, Japan) electrodes has been described.[23] The glassy carbon samples had a diameter of 3 mm. The electrochemical setup was an EG & G 273 A driven by a PC with the M270 software. Potentials are quoted against a saturated calomel electrode (SCE). The counter electrode was platinum gauze of large surface area. All experiments were performed at room temperature.

Catalytic Studies

Materials. All materials were used as purchased without any further purification.

Catalytic Experiments. The four polyanions salts were tested for their heterogeneous catalytic efficiency toward the air oxidation of the two aliphatic and aromatic hydrocarbons *n*-hexadecane and *p*-xylene, respectively. The detailed experimental procedure for each substrate is as follows:

***n*-Hexadecane.** Air oxidation of *n*-hexadecane was carried out in a 25 mL two-necked-round-bottom flask containing 5 mL of fresh substrate and 10 mg of nondissolved catalyst, and then heated to 150 °C with stirring, constant air flow of about 30 mL/min and without the addition of any solvent. After 6 h, the mixture was allowed to cool to ambient temperature, and samples were taken for GC analysis with a flame ionization detector, using a 3900 GC instrument, HP-FFAP column, and He as carrier gas. Substrate loss was below 5% for all the measurements.

***p*-Xylene.** Five milliliters of *p*-xylene, 10 mg of the nondissolved catalyst, and 0.1 g of *tert*-butylhydroperoxide were stirred in a 25 mL 2-necked-round-bottom flask at 130 °C with constant air flow of about 10 mL/min for 12 h. The solution was allowed to cool to ambient temperature, and then the solid product was separated by filtration. The filtrate contained *p*-tolualdehyde, 4-methylbenzyl alcohol, *p*-toluic acid, and unreacted *p*-xylene. The acids formed were esterified using the following procedure: 300 μL of the sample was taken in a glass vial; 2 mL of 14% borontrifluoride (BF_3) in methanol was added to the vial which was sealed with a Teflon lined stopper and heated for 1 h at 80 °C. The sample was cooled to room temperature, and 2 mL of deionized water was added with mild shaking. The esters formed were extracted by the addition of 2 mL of HPLC grade dichloromethane. The lower organic layer containing the product was analyzed by GC. The gas chromatographic analyses were

(22) Sheldrick, G. M. *SADABS*; University of Göttingen: Göttingen, Germany, 1996.

(23) Keita, B.; Girard, F.; Nadjo, L.; Contant, R.; Canny, J.; Richet, M. *J. Electroanal. Chem.* **1999**, *478*, 76.

carried out on a Varian GC 3900-FID using a flame-ionization detector, a VF-1MS column (l = 15 m, ID = 0.25 mm, film thickness: 0.25 μm) and He as carrier gas.

Hot filtration experiments: reactions were performed with the same conditions as described above for *p*-xylene or hexadecane oxidation; however, a 1 mL aliquot was taken from the hot solution after 4 h and transferred to a new vessel containing all starting materials but the catalyst. In this way, any homogeneous contributions to the reaction could be observed by following the progress of the reaction (typically for 3 h) in the second vessel by GC.

Results and Discussion

We have prepared the four (arene)Ru^{2+} (arene = benzene, *p*-cymene) containing polyanions $[Sb_2W_{20}O_{70}(RuC_6H_6)_2]^{10-}$ (**1**), $[Bi_2W_{20}O_{70}(RuC_6H_6)_2]^{10-}$ (**2**), $[Sb_2W_{20}O_{70}(RuC_{10}H_{14})_2]^{10-}$ (**3**), and $[Bi_2W_{20}O_{70}(RuC_{10}H_{14})_2]^{10-}$ (**4**) by one pot reactions between $[Ru(arene)Cl_2]_2$ (arene = benzene, *p*-cymene) and the Krebs-type polyanion precursors $[X_2W_{22}O_{74}(OH)_2]^{12-}$ ($X = Sb^{III}$, Bi^{III}).

The synthesis of **1**−**4** was accomplished by reaction of $[X_2W_{22}O_{74}(OH)_2]^{12-}$ ($X = Sb^{III}$, Bi^{III}) and $[Ru(arene)Cl_2]_2$ in equimolar ratios in sodium acetate buffer medium (pH 6.0). This indicates that the dimeric Ru-precursor is hydrolyzed at such conditions, providing the reactive mononuclear electrophile in situ. Polyanions **1**−**4** were also obtained upon reacting $[Ru(arene)Cl_2]_2$ and $[X_2W_{22}O_{74}(OH)_2]^{12-}$ ($X = Sb^{III}$, Bi^{III}) in higher molar ratios (e.g., 2:1 and 3:1).

Polyanion **3** had already been prepared by Proust's group, albeit through a different route by reaction of $[(C_{10}H_{14})RuCl_2]_2$ with $Na_2WO_4 \cdot 2H_2O$ and Sb_2O_3 instead of $Na_{12}[Sb_2W_{22}O_{74}(OH)_2]$ used in this procedure.[19] On the other hand, we report here the Bi-derivative **4** of Proust's structure, and the benzene derivatives **1** and **2** represent the first examples of lone-pair-containing heteropolytungstates bearing a $Ru(C_6H_6)$ unit. Our group as well as others have already reported some organo-tin derivatives of this class of POMs.[24]

Polyanions **1**−**4** consist of two lacunary *B*-β-$[XW_9O_{33}]^{9-}$ ($X = Sb^{III}$, Bi^{III}) Keggin fragments linked via two inner *cis*-WO_2 groups and two outer (arene)Ru^{2+} units leading to a structure with idealized C_{2h} symmetry (see Figure 1). Alternatively, these polyanions can be described as a dilacunary $[X_2W_{20}O_{70}]^{14-}$ fragment substituted by two (arene)Ru^{2+} units. The structure of **1**−**4** is closely related to the parent structure $[X_2W_{22}O_{74}(OH)_2]^{12-}$ and its transition-metal-substituted derivatives $[X_2W_{20}M_2O_{70}(H_2O)_6]^{(14-2n)-}$ ($X = Sb^{III}$, Bi^{III}; $M^{n+} = Fe^{3+}$, Co^{2+}, Ni^{2+}, Cu^{2+}, Zn^{2+}).[8a,9a,9c] The only difference is that the two outer WO_3 groups in $[X_2W_{22}O_{74}(OH)_2]^{12-}$ and the two transition-metal ions with three aqua ligands each in $[X_2W_{20}M_2O_{70}(H_2O)_6]^{(14-2n)-}$ have been exchanged for (arene)Ru^{2+} in the case of **1**−**4**.

The ruthenium ions in the four polyanions **1**−**4** are bound via an oxygen atom to one $\{XW_9O_{33}\}$ unit, and via two oxygens to the other. Other dimeric organometallic ruthenium containing heteropolytungstates do not exhibit such a binding mode of the Ru center which is most likely dictated by the lone pair repulsion in **1**−**4**. For example, in $[(PW_9O_{34})_2(cis\text{-}WO_2)(cis\text{-}RuL^{Me}{}_2)]^{13-}$ (L^{Me} = 1,3-dimethylimidazolidine-2-ylidene) the ruthenium ion is coordinated to the $\{P_2W_{19}O_{70}\}$ fragment via four Ru−O−W bonds, two to each of the $\{PW_9O_{34}\}$ units.[17] In the case of $[\{PW_{11}O_{39}\{Ru(arene)\}\}_2\{WO_2\}]^{8-}$ (arene = benzene, toluene), each Ru(arene) group is linked to two oxygen atoms of the lacuna and an oxo ligand of the $\{WO_2\}$ group.[18] Nevertheless, the Ru−O(W) distances in **1** to **4** fall in a range comparable to what has been reported for the two above-mentioned polyanions: 2.08(1)−2.09(1) Å for **1**, 2.08(1)−2.10(1) for **2**, 2.08(2)−2.10(2) Å for **3**, and 2.08(2)−2.14(2) Å for **4**. The Ru−O−W angles of the four compounds **1**−**4** are in the range 131.0(7)−177.5(7)° which is larger than 150.3(17)−161.3(17)°, reported for $[\{PW_{11}O_{39}\{Ru(arene)\}\}_2\{WO_2\}]^{8-}$ (arene = benzene, toluene).

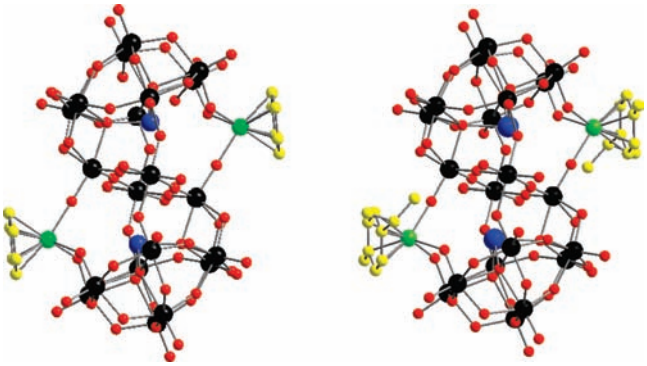

Figure 1. Ball-and-stick representations of polyanions **1** and **2** $[X_2W_{20}O_{70}(RuC_6H_6)_2]^{10-}$ (X = Sb, Bi), left, and polyanions **3** and **4** $[X_2W_{20}O_{70}(RuC_{10}H_{14})_2]^{10-}$ (X = Sb, Bi), right. Color code: black (W), red (O), green (Ru), yellow (C), and blue (Sb or Bi).

Bond-valence sum (BVS) calculations[25] for **1**−**4** indicate that there are no protonation sites and therefore the charge of the polyanions must be −10. In the solid state these charges are balanced by either one or two types of alkali metal ions (sodium, potassium, cesium). Not all sodium ions could be detected by single-crystal XRD because of disorder. However, the presence of the remaining sodium ions was verified by elemental analysis.

We also performed multinuclear solution NMR studies on the diamagnetic polyanions **1**−**4** at room temperature, by dissolving the respective salts **KNa-1**, **CsNa-2**, **CsNa-3**, and **Na-4** in D_2O. The ^{183}W NMR spectra of **1**, **2**, and **4** exhibit the expected six line pattern between −30 and −340 ppm with relative intensities 2:2:2:2:1:1, characteristic of the idealized C_{2h} symmetry of the polyanions (see Figure 2). For **3** we only see five instead of the expected six lines, which is almost certainly because of coincidental overlap of two signals within the set of four intense downfield signals. The signal at −118.8 ppm is in fact significantly more intense than the other two corresponding downfield signals (this is fully consistent with the observations of Proust et al.).[19] Also for polyanion **4** the two central signals are very close, but can still be distinguished (−113.6 and −117.8 ppm). The ^1H- and ^{13}C NMR spectra of **1** and **2** show only one signal, most likely indicating fast rotation of the arene ligands around the C_6 axis in solution which renders all carbons and protons of the two $Ru(C_6H_6)$ groups magnetically equivalent (see Supporting Information, Figures S1 and S2). This phenomenon was also observed for other organo-Ru supported heteropolytungstates.[15a,b,16d,18,19] On the other hand, for **3** and **4** we observed five signals in ^1H NMR and seven signals in ^{13}C

(24) (a) Sazani, G.; Dickman, M. H.; Pope, M. T. *Inorg. Chem.* **2000**, *39*, 939. (b) Hussain, F.; Kortz, U.; Clark, R. J. *Inorg. Chem.* **2004**, *43*, 3237. (c) Hussain, F.; Reicke, M.; Kortz, U. *Eur. J. Inorg. Chem.* **2004**, 2733. (d) Hussain, F.; Kortz, U. *Chem. Commun.* **2005**, 1191.

(25) Brown, I. D.; Altermatt, D. *Acta Crystallogr.* **1985**, *B41*, 244.

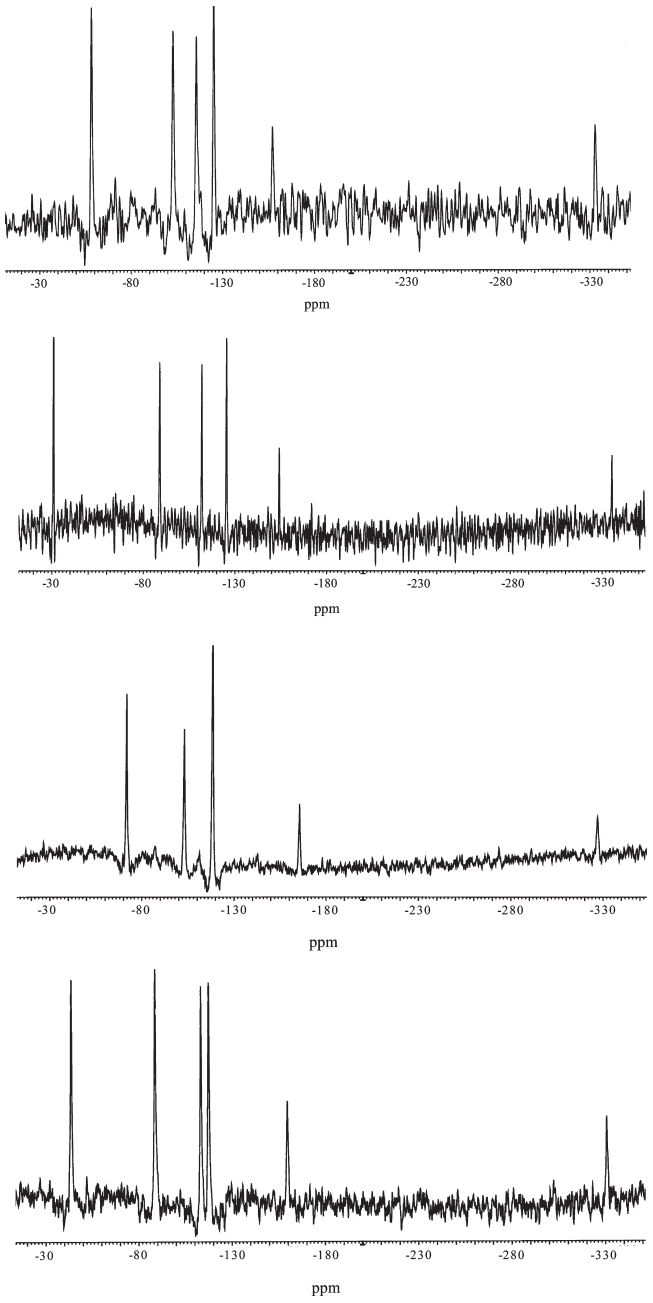

Figure 2. Room temperature ^{183}W NMR spectra of **KNa-1**, **CsNa-2**, **CsNa-3**, and **Na-4** (from top down) redissolved in D_2O.

NMR, which reflects exactly the number of magnetically inequivalent protons and carbons in *p*-cymene. This also implies that fast rotation of the sterically more demanding *p*-cymene (compared to benzene) around the Ru-arene vector is unlikely.

Electrochemistry

In 1998, Krebs' group reported electrochemical studies on $[\{Mn(OH_2)_3\}_2(WO)_2(BiW_9O_{33})_2]^{10-}$, which is structurally related to **1**−**4**.[26] We decided to perform detailed and comparative cyclic voltammetry studies on **1**−**4** to support our catalytic studies (vide infra) and also because the number of stable, isostructural POM families is rare.

The reproducibility of the UV−vis spectra in terms of absorbance and wavelength indicated the stability of the four polyanions **1**−**4** at pH 6 over a period of at least 24 h; **2** and **4** being fairly stable also at pH 3. This stability could also be confirmed by cyclic voltammetry (Supporting Information, Figure S3).

For simplicity and ease of comparison, the choice was made to describe separately the respective electrochemical behaviors of the W-centers and the Ru-centers in **1**−**4**. Table 2 gathers the main voltammetric characteristics of the first W-wave for each polyanion. Figure 3A shows in superposition the W-waves obtained for **1** and **2** in pH 6 medium. Before the solvent cathodic limit, two well-behaved waves are observed for **1** while only one slightly drawn-out voltammetric pattern is obtained for **2.** This single wave is followed by an ill-defined small shoulder. The formal redox potentials and the anodic-to-cathodic peak potential differences in Table 2 call for the following remarks. The redox potential in the case of the Bi-derivative **2** is more negative than that of its Sb analogue **1.** Although the structures of the present polyanions are different from those of the more frequently described P^V- and As^V-based POMs, a tentative analogy might be made with them. Generally, the W-waves are located at less negative potential in the As-group of polyanions than in the P-group. The present result corresponds to the reverse of this expectation. However, two parameters should be taken into account to explain this observation. The anodic to cathodic peak potential differences in Table 2 indicate the overall charge transfer to be faster for the Sb-derivative **1**. In-line with this observation, the peak current intensity is smaller for the Bi-derivative **2**. The same arguments can be made for the other, cymene-based pair **3** and **4.** The cyclic voltammogram of **2** in the pH 3 medium could be run, because of the stability of the polyanion. The voltammetric pattern is shown in Supporting Information, Figure S3, in superposition with that obtained at pH 6. The pH 3 wave is well-behaved with a larger peak current intensity than at pH 6. This result suggests the relative slowness of the overall charge transfer in the pH 6 medium to be attributable to the low proton availability.[27] Following this line of reasoning, it might be inferred that **1**−**4** have very different pK_a values, with reduced **1** being the most basic, thus permitting the observation of two well-developed voltammetric waves at pH 6. In the pH 6 acetate medium, exploration of the potential domain up to 1.3 V versus SCE for polyanion **2** shows the pattern illustrated in Figure 3B superimposed with that of the supporting electrolyte alone as a reference, indicating that in addition to the Ru(arene) fragment related processes, there occurs also a strong water oxidation process at a more positive potential. This important process has been investigated before in POM chemistry.[28] Because of its importance, a detailed study of this catalytic reaction is planned but is beyond the scope of the present paper. These conclusions are reinforced by the electrochemical pattern obtained for the Ru-precursor $[(C_6H_6)RuCl_2]_2$, which displays a chemically irreversible oxidation pattern analogous to that of **2**, except for a less

(26) Bösing, M.; Nöh, A.; Loose, I.; Krebs, B. *J. Am. Chem. Soc.* **1998**, *120*, 7252.

(27) Keita, B.; Lu, Y.-W.; Nadjo, L.; Contant, R. *Eur. J. Inorg. Chem.* **2000**, 2463.

(28) (a) Howells, A. R.; Sankarraj, A.; Shannon, C. *J. Am. Chem. Soc.* **2004**, *126*, 12258. (b) Quinonero, D.; Wang, Y.; Morokuma, K.; Khavrutskii, L. A.; Botar, B.; Geletii, Y. V.; Hill, C. L.; Musaev, D. G. *J. Phys. Chem. B* **2006**, *110*, 170. (c) Keita, B.; Mialane, P.; Sécheresse, F.; de Oliveira, P.; Nadjo, L. *Electrochem. Commun.* **2007**, *9*, 164.

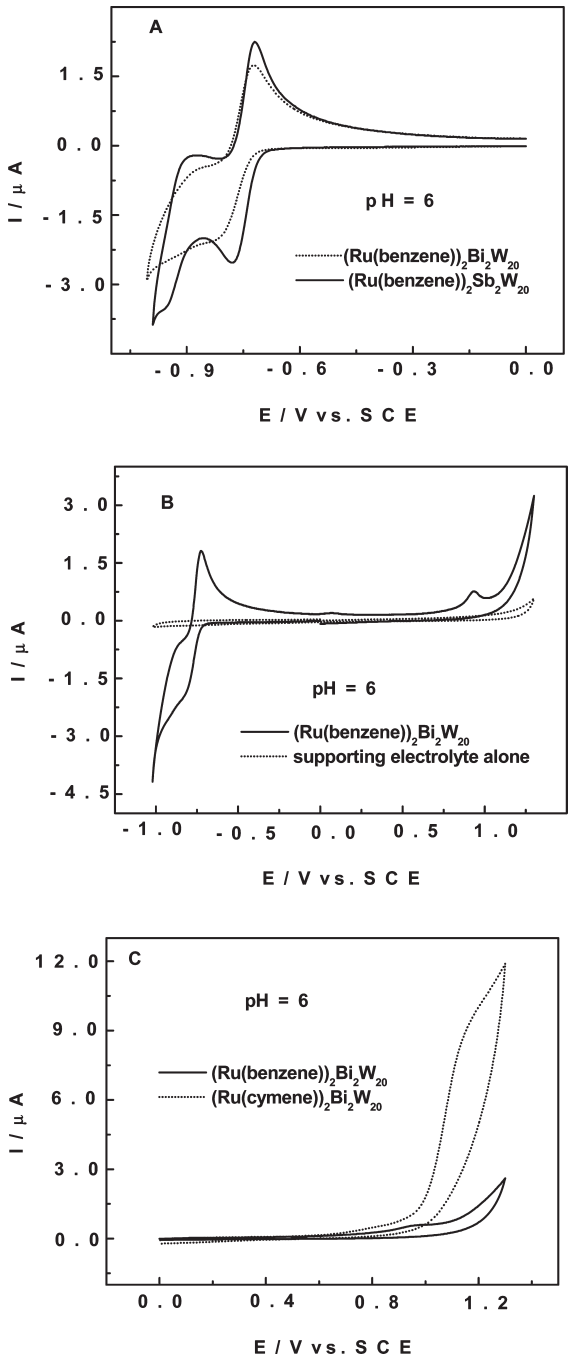

Figure 3. Cyclic voltammograms of 2×10^{-4} M **1**, **2**, and **4** in a pH 6 medium (0.4 M CH_3COONa + CH_3COOH). The working electrode was glassy carbon and the reference electrode was SCE. The scan rate was 10 mV s^{-1}. (A) The voltammetric patterns for **1** and **2** are restricted to the W-redox processes. (B) Superposition of cyclic voltammograms of the pH 6 electrolyte and of **2** showing both the anodic and cathodic processes. (C) Superposition of the cyclic voltammograms of **2** and **4** with restriction to the oxidation processes.

favorable water oxidation process. A detailed study of this reactant is, however, beyond the scope of the present communication. Schematically, between +0.6 V and +1.3 V versus SCE, the oxidation process of the Ru(benzene) fragment within **2** is featured by one clearly defined wave followed by a very high current intensity process attributed to electrocatalytic water oxidation. The well-defined oxidation wave has no separated cathodic counterpart up to the

Table 2. Main Characteristics of the First W-Wave for **1**−**4** in pH 6 Medium[a]

polyanion	$-E^b$ / V vs SCE	ΔE^c / V
$[Sb_2W_{20}O_{70}(RuC_6H_6)_2]^{10-}$ (**1**)	0.748	0.056
$[Bi_2W_{20}O_{70}(RuC_6H_6)_2]^{10-}$ (**2**)	0.772	0.096
$[Sb_2W_{20}O_{70}(RuC_{10}H_{14})_2]^{10-}$ (**3**)	0.754	0.052
$[Bi_2W_{20}O_{70}(RuC_{10}H_{14})_2]^{10-}$ (**4**)	0.773	0.070

[a] Scan rate: 10 mV s^{-1}. For further details, see text. [b] $E°$ is defined as the average of the cathodic and anodic peak potentials. [c] ΔE is the anodic to cathodic peak potentials difference.

W-reduction process. This pattern is observed whatever the direction of the initial scan. The same observations were made for polyanion **1**. It was even possible to demonstrate the stepwise oxidation of **2** in pH 3 medium (Supporting Information, Figure S4).

The study of **3** and **4** in the pH 6 medium (Supporting Information, Figure S5), leads to the same conclusions as for their benzene analogues **1** and **2**. Unfortunately, resolution of the oxidation into separate steps could not be achieved because the cymene-derivatives were not stable in pH 3 medium. Here, polyanion **4** in the pH 6 medium is found to be more difficult to be oxidized by some 50 mV than **3**, in agreement with our rough expectation. The benzene derivatives **1** and **2** behave similarly. Figure 3B compares the cyclic voltammograms of **2** and **4** in the pH 6 medium, to highlight the differences brought about by the two different arene ligands. It appears from Figure 3B that the oxidation peak potentials attributed to the Ru(arene) fragment are nearly the same for the two polyanions (0.930 V vs 0.940 V, respectively) in agreement with the small expected electronic effects. Both of these potentials are distinctly less positive than that observed for the Ru-precursor $[(C_{10}H_{14})RuCl_2]_2$ which is observed at 1.00 V versus SCE in the pH = 6 medium, highlighting a larger electronic effect. However, the voltammograms of **2** and **4** can be easily distinguished from each other: the catalytic activity of the two complexes, evaluated through the current intensities for water electrocatalytic oxidation, is strikingly larger for **4** (Figure 3C). In addition, the Ru-precursor $[(C_{10}H_{14})RuCl_2]_2$ shows no catalytic activity in the potential domain where **2** and **4** are active. The same observation was made for the Sb-derivatives **1** and **3.** In contrast to the expected lack of influence of benzene or cymene on the electrochemistry of the W-centers in **1**−**4**, the behavior observed for the oxidation processes can be considered as a distinctive fingerprint for each of the two arene ligands. Cyclic voltammetry established unambiguously that polyanions **1**−**4** are promising candidates for catalytic water oxidation. Future work will focus on analytical and quantitative aspects of this oxidation including large scale bulk electrolyses.

Catalytic Studies. ***n*-Hexadecane.** The catalytic activity of the polyanion salts **KNa-1**, **CsNa-2**, **CsNa-3**, and **Na-4** toward air oxidation of hexadecane was investigated. Table 3 summarizes the percent conversion of substrate after heating at 150 °C for 6 h, turnover frequency (TOF) and selectivity for ketone and alcohol formation. *n*-Hexadecane was oxidized only at the secondary C−H bonds to afford mainly the corresponding ketones. Primary C−H bonds could not be oxidized. The isostructural "all-tungsten" derivatives $Na_{12}[Sb_2W_{22}O_{74}(OH)_2]\cdot 44H_2O$ (**Sb_2W_{22}**) and $Na_{12}[Bi_2W_{22}O_{74}(OH)_2]\cdot 44H_2O$ (**Bi_2W_{22}**), which are the synthetic precursors of

Table 3. Catalytic Activity of the Four Ru-POM Catalysts for *n*-Hexadecane Air Oxidation[a]

			product selectivity (mol %)[d] and distribution	
catalysts	*n*-$C_{16}H_{34}$ Conv. (mol %)[b]	TOF[c] (h^{-1})	ketones (7-one:6-one:5-one:4-one:3-one:2-one)[e]	alcohols (7-ol:6-ol:5-ol:4-ol:3-ol:2-ol)[f]
blank	3.9	-	55	24
Sb_2W_{22}	9.5	177	53 (32:9:10:12:14:23)	21(16:19:27:17:0:21)
Bi_2W_{22}	6.3	121	52 (33:10:11:13:15:18)	22 (20:14:26:17:0:23
KNa-1	38.3	636	52 (40:10:12:15:16:7)	22 (23:8:12:24:8:25)
CsNa-2	33.7	570	50 (38:10:15:14:16:7)	29 (21:8:9:27:6:29)
CsNa-3	34.0	605	51 (40:11:12:16:9:12)	25 (24:8:10:25:7:26)
Na-4	31.8	570	50 (40:12:13:16:8:11)	23 (25:9:10:23:6:27)

[a] Reaction conditions: 10 mg of catalyst, 5 mL (3.875 g) of *n*-hexadecane, airflow rate 30 mL/min, temperature 150 °C, reaction time 6 h. [b] *n*-C_{16} conv. (%) = (reacted *n*-hexadecane/introduced *n*-hexadecane) × 100. [c] TOF = moles of *n*-hexadecane converted per mole catalyst per hour. [d] Product selectivity: ketones or alcohols (%) = produced ketones or alcohols/reacted *n*-hexadecane. [e] 7-one = 7-hexadecanone, 6-one = 6-hexadecanone, 5-one = 5-hexadecanone, 4-one = 4-hexadecanone, 3-one = 3-hexadecanone, 2-one = 2-hexadecanone. [f] 7-ol = 7-hexadecanol, 6-ol = 6-hexadecanol, 5-ol = 5-hexadecanol, 4-ol = 4-hexadecanol, 3-ol = 3-hexadecanol, 2-ol = 2-hexadecanol.

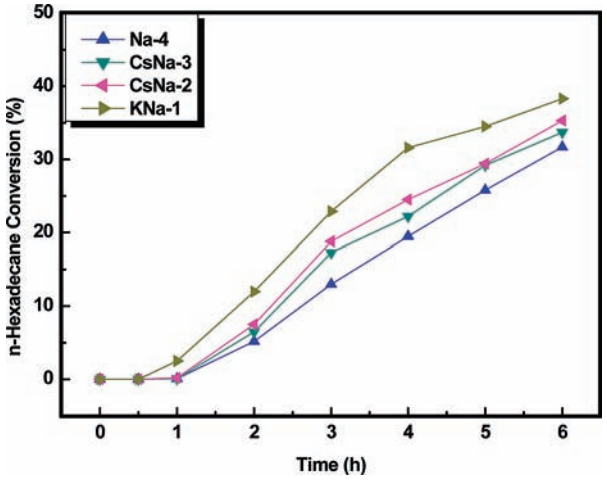

Figure 4. Comparative time profiles for the oxidation of *n*-hexadecane using the four different Ru-POM salts as catalysts.

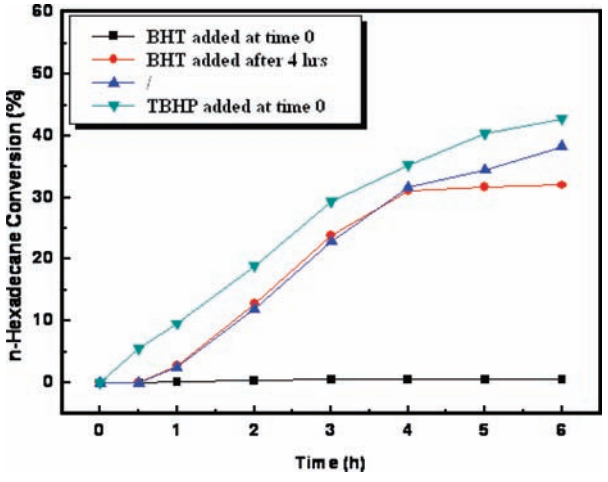

Figure 5. Time profile of air oxidation of *n*-hexadecane using **KNa-1** as a catalyst (blue upright triangles), with the addition of TBHP initiator at the beginning (green inverted triangles), with the addition of BHT radical scavenger at the beginning (black squares) and with the addition of BHT after 4 h of the reaction (red circles).

the Ru-POMs, were not catalytically inactive as compared to the blank control experiment in which air was bubbled through the substrate alone. Ruthenium substitution of tungsten, however, greatly increased the catalytic activity. With **KNa-1** as catalyst we observed 38.3% conversion of *n*-hexadecane with 52% selectivity toward ketones and 22% selectivity toward alcohols. All four POMs showed almost the same selectivity to C_{16} ketones (ca. 50%) and C_{16} alcohols (ca. 24%) and a narrow range of *n*-hexadecane conversion to different oxidation products, with **KNa-1** being the best catalyst with no significant variation in performance of the four compounds. More significantly, the TOF and the conversion values were more than 10 times higher than those reported by us for the selective oxidation of *n*-hexadecane with air catalyzed by unsupported iron substituted polytungstates.[29] Additionally, the conversion percentages for the Ru-POMs in question are slightly higher than the values reported in a study done on the $[Cu_{20}Cl(OH)_{24}(H_2O)_{12}(P_8W_{48}O_{184})]^{25-}$ (**Cu_{20}**) polyanion on the same oxidation reaction following the same systemized method, with the only difference that **Cu_{20}** is supported on 3-aminopropyltriethoxysilane (apts) modified SBA-15. The turnover frequency, however, is ~20 times higher in the case of **Cu_{20}**.[30] Further, hot filtration experiments were performed by removing 1 mL aliquots from the hot reaction after 4 h and added to a fresh solution of hexadecane under identical reaction conditions but without catalyst. In all cases here, no further reaction was observed in the second reaction vessel thus implying no homogeneous species contributes to the catalytic activity. Additionally, the Ru precursor materials $[(C_{10}H_{14})RuCl_2]_2$ and $[(C_6H_6)RuCl_2]_2$ exhibited conversions of 8.2 and 7.8%, respectively.

Simultaneous hydrocarbon combustion took place as evidenced by the formation of lower carbon chain (mainly C6−C13) carboxylic acids (ca. 12%). The other trace compounds of the product mixture were found to be aldehydes, paraffins, and ketones with less than 10 carbon atoms.

To follow the course of the reaction with the four Ru-POMs salts over the period of 6 h, analysis of the products was performed for each at different time intervals, 0.5, 1, 2, 3, 4, 5, and 6 h (Figure 4). The figure shows that conversions increased linearly with time after a certain induction period (0.5 h for **1** and 1 h for **2**−**4**).

(29) Chen, L.; Zhu, K.; Bi, L. H.; Suchopar, A.; Reicke, M.; Mathys, G.; Jaensch, H.; Kortz, U.; Richards, R. M. *Inorg. Chem.* **2007**, *46*, 8457.

(30) Chen, L.; Hu, J.; Mal, S. S.; Kortz, U.; Jaensch, H.; Mathys, G.; Richards, R. M. *Chem.—Eur. J.* **2009**, *15*, 7490.

Table 4. Catalytic Activity of the Four Ru-POM Catalysts for *p*-Xylene Air Oxidation[a]

			product selectivity (mol %)[d] and distribution		
catalysts	C_8H_{10} conv. (mol %)[b]	TOF[c] (h^{-1})	A[e]	B[f]	C[g]
blank	0.1		0	100	0
Sb_2W_{22}	0.7		59	41	0
Bi_2W_{22}	1.4		58	42	0
KNa-1	12.1	1333	59	17	25
CsNa-2	13.5	587	61	26	13
CsNa-3	15.9	1431	70	16	13
Na-4	14.0	360	67	20	13

[a] Reaction conditions: 10 mg of catalyst, 5 mL of *p*-xylene, 0.1 g of TBHP, airflow rate 10 mL/min, temperature 130 °C, reaction time 12 h. [b] *p*-xylene conv. (%) = (reacted *p*-xylene /introduced *p*-xylene) × 100. [c] TOF = moles of *p*-xylene converted per mole catalyst per hour. [d] Product selectivity: nb of mole of product/reacted *p*-xylene. [e] *p*-Methyl benzyl alcohol. [f] *p*-Tolualdehyde. [g] *p*-Toluic acid.

Figure 5 demonstrates the effect of a radical initiator and inhibitor on the reaction, using **KNa-1** as the catalyst. Comparing the reaction kinetic profiles in the presence (inverted triangles) and absence (upright triangles) of TBHP (7% *tert*-butyl hydroperoxide) clearly shows that the addition of a free radical initiator greatly reduced the initial induction period, accelerated the rate of the reaction, and gave rise to enhanced activity. On the other hand, addition of a small amount of the free radical scavenger BHT (3,5-tertbutyl-4-hydroxytoluene), completely suppressed the substrate conversion, whether at the beginning of the reaction (squares) or after a certain time interval such as 4 h (circles). These observations lead to the conclusion that the Ru-POMs-catalyzed air oxidation of *n*-hexadecane clearly involves a free radical mechanism. Similar results have been observed for other transition metal catalyzed oxidations of alkanes such as cyclohexane,[31] where the formation of the peroxide intermediate has been explicitly detected.

***p*-Xylene.** The same four Ru-POM salts **KNa-1**, **CsNa-2**, **CsNa-3** and **Na-4** were tested as catalysts for the solvent free oxidation of *p*-xylene. As products we observed mainly *p*-methyl-benzylalcohol, *p*-tolualdehyde, and *p*-toluic acid. No evidence for the formation of the fully oxidized terephthalic acid was found throughout these experiments. Table 4 summarizes the results of the performance of the four Ru-POM catalysts together with the two "all-tungsten" derivatives **Sb_2W_{22}** and **Bi_2W_{22}** and the blank corresponding to the substrate alone. **Sb_2W_{22}** and **Bi_2W_{22}** resulted in significantly lower substrate conversions, emphasizing the importance of the ruthenium centers for the catalytic activity. The range of conversions exhibited by the use of the five Ru-POMs is 12 to 16%, with **CsNa-2** being the catalyst with the highest-conversion. **KNa-1**, in contrast, showed the lowest conversion but the best selectivity for *p*-toluic acid. The main oxidation product of *p*-xylene was, in general, the alcohol with selectivity of 60 up to 70% in some cases. It is also worth noting that the TOFs for the benzene-containing polyanion salts **KNa-1** and **CsNa-2** were higher than those of the corresponding *p*-cymene derivatives **CsNa-3** and **Na-4**. Again, hot filtration experiments were performed for all catalysts and no further reaction was observed in the second reaction vessel. The Ru precursor materials $[(C_{10}H_{14})RuCl_2]_2$ and $[(C_6H_6)RuCl_2]_2$ exhibited conversions of 4.6 and 3.6%, respectively. The reactions without catalyst in the presence and absence of TBHP initiator provided only 0.1 and 0% conversions, respectively.

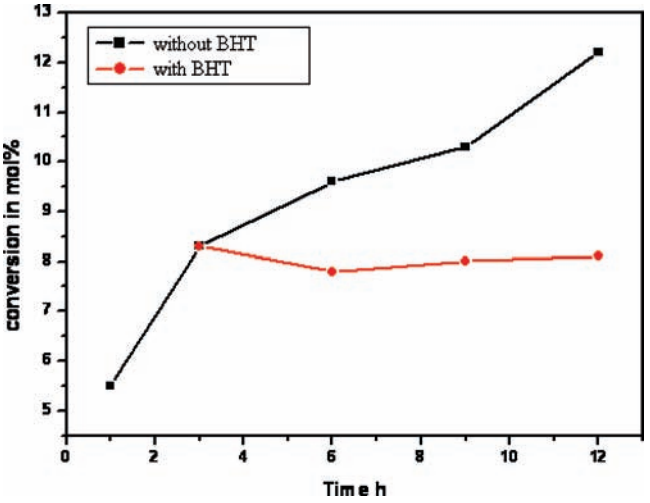

Figure 6. Time profile of air oxidation of *p*-xylene using **KNa-1** as a catalyst (black squares) and with the addition of BHT after 3 h of the reaction (red circles).

The effect of a radical scavenger (BHT) on the reaction route was assessed and the results are presented in Figure 6. We observed the complete suppression of substrate conversion upon addition of BHT. Furthermore, the yields were very low when the reaction was conducted without addition of TBHP, indicating that the reaction most likely proceeds via a free radical mechanism. Under the reaction conditions, the TBHP initiator is expected to abstract a hydrogen from the methyl group of *p*-xylene which forms a peroxo radical that further reacts to give the final products.

The time profiles for the reactions using the Ru-POM salts **KNa-1**, **CsNa-2**, **CsNa-3**, and **Na-4** are shown in Supporting Information, Figure S6. For each POM, five reactions were started simultaneously and each was stopped after a different time interval: 1, 3, 6, 9, and 12 h, respectively, followed by subsequent GC-analysis of the products. The graph shows that the conversion increases linearly with time, without induction period because of the presence of the radical initiator. All four POMs maintained their structures after the reactions, as shown by separation of the POM salt and consecutive IR analysis.

Conclusions

We have synthesized and structurally characterized four organo-Ru supported lone pair containing heteropolytungstates.

(31) (a) Sankar, G.; Raja, R.; Thomas, J. M. *Catal. Lett.* **1998**, *55*, 12. (b) Modén, B.; Zhan, B. Z.; Dakka, J.; Santiesteban, J. G.; Iglesia, E. *J. Catal.* **2006**, *239*, 390.

The polyanions $[X_2W_{20}O_{70}(RuL)_2]^{10-}$ (X = Sb^{III}, L = benzene, **1**; X = Bi^{III}, L = benzene, **2**; X = Sb^{III}, L = *p*-cymene, **3**; X = Bi^{III}, L = *p*-cymene, **4**) consist of two $(L)Ru^{2+}$ units linked to a Krebs-type polyanion $[X_2W_{20}O_{70}]^{14-}$ fragment resulting in an assembly with idealized C_{2h} symmetry. Polyanions **2** and **4** represent the first structurally characterized organo-Ru supported heteropolybismuthates(III). Polyanions **1**−**4** were characterized by FT-IR, UV−vis, thermogravimetric analysis, multinuclear solution NMR spectroscopy (^{183}W, ^{13}C, ^{1}H), single-crystal X-ray diffraction, and elemental analysis.

Our electrochemical studies on **1**−**4** indicated that the central heteroatom X influences the reduction potentials of the W-centers. On the other hand, the nature of the arene in the Ru(arene) fragments has practically no influence on the formal reduction potentials of the W-centers, though the influence can be clearly detected in the case of oxidation processes where the identity of the arene can be accordingly specified. A strong electrocatalytic water oxidation process is also worth pointing out.

We have also conducted oxidation reaction studies using the four organo-ruthenium polyanions as heterogeneous catalysts and *n*-hexadecane and *p*-xylene as substrates. For all four ruthenium-containing polyanions the yields were comparable, independent of the substrate, and significantly higher than for the blank and the corresponding "all-tungsten" derivatives $\mathbf{Sb_2W_{22}}$ and $\mathbf{Bi_2W_{22}}$. This is evidence suggesting the importance of the ruthenium centers on the overall catalytic efficiency of the POMs for this type of reactions.

Acknowledgment. U.K. thanks ExxonMobil, the Fonds der Chemischen Industrie, and Jacobs University for research support. R.R. thanks Jacobs University and the Colorado School of Mines for research support. Figure 1 was generated by Diamond Version 3.2c (copyright Crystal Impact GbR). This work was also supported by the CNRS and the University Paris−Sud 11 (UMR 8000).

Supporting Information Available: Crystallographic data in CIF format and additional information as noted in the text. This material is available free of charge via the Internet at http://pubs.acs.org.